IEEE Access
Multidisciplinary ⋮ Rapid Review ⋮ Open Access Journal

Received 9 February 2023, accepted 3 March 2023, date of publication 10 March 2023, date of current version 16 March 2023.
Digital Object Identifier 10.1109/ACCESS.2023.3255780

RESEARCH ARTICLE

Design and Performance Analysis of Ultra-Wide Bandgap Power Devices-Based EV Fast Charger Using Bi-Directional Power Converters

TEHSEEN ILAHI[1,2], TAHIR IZHAR[1,3], SAEED MIAN QAISAR[4,5,6], UMAR TABREZ SHAMI[1], MUHAMMAD ZAHID[2], ASAD WAQAR[7], AND AHMAD ALZAHRANI[8]

[1]Department of Electrical Engineering, University of Engineering and Technology (UET) Lahore, Lahore 54890, Pakistan
[2]Department of Electrical Engineering, Riphah International University, Lahore 54000, Pakistan
[3]Research and Development, Maxell Power, Pvt. Ltd., Lahore 54000, Pakistan
[4]Department of Electrical and Computer Engineering, Effat University, Jeddah 22332, Saudi Arabia
[5]Communication and Signal Processing Laboratory, Energy and Technology Research Center, Effat University, Jeddah 22332, Saudi Arabia
[6]LINEACT CESI, 69100 Lyon, France
[7]Department of Electrical Engineering, Bahria School of Engineering and Applied Sciences, Bahria University, Islamabad 44000, Pakistan
[8]Department of Electrical Engineering, College of Engineering, Najran University, Najran 11001, Saudi Arabia

Corresponding authors: Tehseen Ilahi (tehseen.ilahi@riphah.edu.pk) and Asad Waqar (asadwaqar.buic@bahria.edu.pk)

This work was supported in part by the Deanship of Scientific Research at Najran University through the Research Collaboration Funding Program under Grant NU/RC/SERC/11/1, and in part by Effat University under Grant UC#9/2June2021/7.2-21(3)5.

ABSTRACT A widespread introduction of electric vehicles would require an advanced enriched fast-charging infrastructure and battery technology. Currently used silicon (Si) based power electronic devices limit their efficiencies, power density, and switching frequency. Designing fast-charging stations using these materials is not suitable due to low breakdown potential, less thermal stability, and less power handling abilities. The research will propose an off-board DC high-power density fast charging infrastructure with grid tie application. The EV station is designed by using ultra-wideband gap (UWBG) material-based power electronic devices to charge the EV vehicles in a few minutes up to an acceptable state of charge. The study will analyze the characteristics of Gallium III oxide (Ga_2O_3) material power devices by modeling them using SPICE and TCAD software tools. The research presents the Simscape physical modeling of electric vehicle chargers based on Ga_2O_3 power devices. Design analysis of three-phase bidirectional AC/DC converter and DC/DC isolated full bridge converter is present in this paper. Research implements the unity power factor control to improve the power quality requirements of the power grid. The dual active power control of converters provides a wide range of charging power for a variety of EV batteries. The study will provide high current and reliable rapid charging for currently available and upcoming future electric vehicles.

INDEX TERMS Ultra-fast electric vehicle DC charger, Ga_2O_3 material power devices, AC/DC power converter, DC/DC isolated converter, TCAD device simulation, Simscape model, loss analysis.

I. INTRODUCTION

Energy-efficient technology and power management are tremendous problems in today's world [1]. In past decades there has been a substantial change from fuel to electric-based automobile transportation. Vehicles are reshaping the comfort of human society for a long time. In today's modern era fast and efficient transportation facility is a necessity [2]. An astonishing fact about the EV is that the electric-driven vehicle was developed earlier than internal combustion engine (ICE) automobiles [3]. Conventional vehicles induce environmental and pollution problems that are harmful to human life [4], [5]. Electric vehicles (EV) or battery electric vehicles (BEV) can diminish greenhouse emissions and hence pollution problems can be controlled [6], [7]. The progressive tendency in electric cars commonly known as battery electric vehicles (BEV), electric vehicles (EV), hybrid electric vehicles (HEV), and Plug-in

The associate editor coordinating the review of this manuscript and approving it for publication was Salvatore Favuzza.

HEV (PHEV) tends to reduce fuel usage and environmental pollution [8]. Advanced countries like the USA have domestic intent to introduce more than 1 million BEV or EVs on road by 2020. They have implemented public policies of electrification at the government level. Major hurdles of EVs comprise cost, battery life, charger limitation, and deficiency of charging infrastructure [9]. Modern countries are promoting the traditional infrastructure of direct current charging systems to support EVs. These systems include the typical power station of 50-120 kW [10].

The rapid expansion of EV manufacturing mandates a comparable development of fast and high-power charging facilities. Typically storage battery charging system contains a DC-DC converter and power factor correction circuit [11]. Figure 1 shows the general block diagram of the electric vehicle charging infrastructure consisting of different bi-directional power converters.

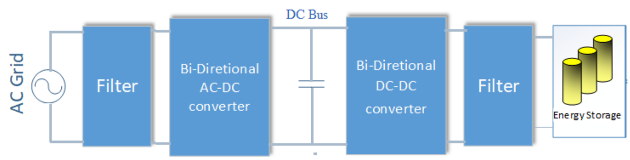

FIGURE 1. General bi-directional EV charging topology.

Traditional EV plug-in charging system recharges the vehicles overnight. These home-based charging systems are not most testimony stations as they are lacking in power capacity, metering, and quality issues and may require additional circuits. Some venture introduces commercial charging at parking lots which provide additional infrastructure for EV users [12]. Even with the availability of these stations, charging time and availability of power are still issues. Different battery capacities and ranges of some PHEVs and EVs are shown in Table 1.

TABLE 1. Battery capacity and range of some PHEV and EV.

Serial No.	Vehicle/ Category	Battery type and energy capacity	Electrical range
1	Toyota [9] PHEV	Li-Ion 4 kWh	10-15 miles
2	Chevrolet PHEV	Li-Ion 16kWh	35-40 miles
3	Mitsubishi EV	Li-Ion 16kWh	80-96 miles
4	Nissan EV	Li-Ion 25kWh	100 miles
5	Tesla [9] Model S EV	Li-Ion 100kWh	245 miles
6	Tesla Founders Series EV	Li-Ion 200kWh	620 miles

Charging stations can be categorized into three levels depending on the power levels and charging scheme. Level 1 is typically a slow charger with a power level of 1.4 to 1.9 kW. Use a standard supply level of 120V/15A single-phase plug. Level 2 is also an on-board system like level 1 with a power capacity of 4 to 19.2 kW that can be charged EV in both ac and dc modes. Level 3 is a fast and high-power charger having a capacity of 50 to 100kW or more [13]. EV chargers can be divided into two types ON board and OFF board chargers. ON board system uses the direct link between the charger inlet and connector (the charging system is inside the vehicle) while the Off-board charger is designed for high power and installed outside the vehicle [14]. Three-phase bidirectional multilevel converters are recommended for high-power Level 3 charger systems. Level 3 commercial fast charging offers the possibility of charging in less than 1 h. It can be installed in highway rest areas and city refueling points, analogous to gas stations. It typically operates with a 400-420V or higher three-phase circuit and requires an off-board charger to provide regulated ac–dc conversion.

It is extensively believed that an acceptable charging facility is ground for the growing EV market [15]. In reference [16] author provides a numerical model of electric car charging needs for a growing charging station. Fang He and others study in [17] modelling framework which monitors the communication among public charging accessibilities and the cost of electricity. Chevy bolt-2018 vehicle with 60 kW Li-ion battery having a driving range of nearly 235 miles takes 75 minutes while charging from the super-fast station of 50kW [18]. The recent improvement in fast charging stations charges up to 80% typical 25kW battery vehicle within 30 minutes [19]. Boicea [20] explains the overview of present energy storing methods including batteries, flywheels, supercapacitors, superconducting magnetic energy storage, and more. The result of [21] shows that a battery buffering unit of nearly 4 to 7 % of maximum power rating can be useful to reduce output fluctuation to under 10%. Since technologies for charging and discharging of the EVs batteries have advanced, the issue of electricity exchange between EVs and the power grid (G2V & V2G) has come to the attention of the public. The stability of the power system and the operation of the power market are significantly impacted by the charging and discharging behaviors of EVs. With blockchain, the power grid can handle dispersed energy more efficiently. V2G operation may cause battery degradation and require other services like frequency regulation, dispatch of the economic revenue, specific protocols, and variables that should be considered while V2G operation [22], [23]. Moreover, EV charger increases the demand and pressure on the power grid causing dangerous effects on the distribution side. Renewable integrated EV systems will reduce the demand for power grid systems and decrease fossil fuel-based energy generation [24], [25].

The Fast-charging station uses power electronic converters to charge electric vehicles. Present technology uses silicon-based power electronic devices which limit their efficiencies and switching frequency up to nearly 30kHz. Designing fast-charging stations using these materials is not suitable due to low breakdown potential, less thermal stability, and less power handling abilities. DC-DC and AC-DC converters experience very high voltage stress and reduce system efficiency. Silicon-based IGBT has a limitation of a maximum potential of nearly 6 kV [26]. The current situation needs new substances to combat increasing demands. The research groups look to the next generation of power semiconductor materials called ultra-wideband gap (UWBG) materials having an energy gap of nearly 6eV. Commonly UWBG materials are AlGaN, AlN, Ga_2O_3, and cubic BN (c-BN) [27].

Wide bandgap semiconductor (WBGs) devices handle a few kilovolts (kV) of potential. WBG material-based devices intensively improve the power density of approximately 50W/in^3 and efficiencies as well. ABB and Tesla introduced their latest DC fast charger with 350kW and 150kW charging capacities [28]. The charging efficiency increases up to 95%. The WBG technology-based SiC MOSFET is introduced which can handle current up to 100A but for upcoming battery and vehicle technology still, high-power handling power devices are required. WBGs SiC MOSFETs have encountered low channel mobility, poor gate oxide accuracy, and catastrophic breakdown problem at high potential. UWBG materials have demonstrated a breakdown voltage of VB > 8 kV, a critical field strength of 8 MV/cm, current density of approximately 3.5 kA/cm^2, remarkably low gate leakage current, and figure of merit (FOM) of nearly 150 MW/cm^2 [29], [30]. UWBG devices also have many other advantages like less switching transient, reduced overall size, fewer conduction losses, cutting down voltage and current stress, and efficiency. These devices will be able to handle hundreds of kV potential and can be operated at a higher frequency. Soft switching techniques can be eliminated in UWBG devices. Ga_2O_3 (UWBG) power devices are not commercially matured to be compared in terms of economics. However, the material Ga_2O_3 has advantages for device development from a perspective of economic cost due to its easy availability [31], [32]. These materials have a better figure of merits (FOM) and performance as compared to WBG materials [33], [34].

The study focuses on designing aspects of high-density DC fast chargers using efficient power devices. Most of the previous work is done on WBG devices-based DC EV fast chargers. In this research high power charger is discussed and simulated using a physical modeling tool (Simscape, MATLAB) designed by UWBG power devices is presented. UWBG (Ga_2O_3) device MATLAB (SPICE model) performance is further compared with Silvaco TCAD results to validate the model behavior. The simulation analysis is performed on a Li-Ion 100kWh capacity battery (nearly the same capacity is used in the latest 2022 EV e.g Mercedes EQS, Ford Mustang Mach-E, Tesla Model S, etc.). The ultra-fast charger proposed in research using UWBG power devices will be able to charge EVs at higher efficiency compared to the present technology. Also, due to considerable breakdown strength, it can be easily useable for direct Grid-tie applications.

The novelty of this research is to observe the high efficiency of power converters using UWBG-based power devices. Modeling analysis of high-capacity EV chargers designed using these converters. The study proposed an ultra-fast 500kW EV charger topology for upcoming high-density EV battery technology. In section II, the Gallium (III) trioxide (Ga_2O_3) material-based power device characteristics curve is evaluated using TCAD and the SPICE paraments are extracted. Section III discussed the modeling of AC/DC & DC/DC power converters for high-power EV fast chargers including mathematical equations used for the design procedure. The Simscape physical modeling and results are presented in section IV. In section V, the conduction & switching power loss analysis is performed and a quantitative comparison with a silicon carbide (SiC) device is evaluated. The proposed topology and its performance parameter evaluation with a commercial EV charger are summarized. At the end research summary and conclusion of the research are presented.

II. MODELING AND PERFORMANCE ANALYSIS OF Ga_2O_3(UWBG) POWER DEVICE

Gallium (III) trioxide (Ga_2O_3) material power devices gain much popularity for future generation power electronics due to their high Baligas figure of merit (BFoM) which shows how much material is compatible with power utilization. The electric field strength of Ga_2O_3 (UWBG) is three times more than that of Silicon carbide (SiC) technology which is related to the wide bandgap (WBG) category [35]. In this research modeling of Ga_2O_3 power, devices are illustrated briefly since fabrication is not the primary objective of the study. The parameter used in this research to evaluate the performance of Ga_2O_3 device is summarized in Table 2.

TABLE 2. Parameters used in TCAD for Ga.

Sr. No	Parameter	value
1	Band Gap Energy	4.8 eV
2	Electron Affinity	4.0 eV
3	Electron Mobility (με)	118 cm^2/V·s
4	Effective density (Nc) (conduction band at 300 K)	3.72 ×10^{18} cm^{-3}
5	Relative permittivity (εs)	10

Silvaco TCAD (technology computer-aided design) is used for performance analysis of Ga_2O_3 semiconductor devices. TCAD has been proven to be a powerful tool to provide an in-depth understanding of device fabrication and operation. The device is constructed with a thick epitaxy layer(100nm) of Ga_2O_3 material with a dopant concentration of 2×10^{17}cm^{-3}. The depth of drain and source area of the power device is kept at 50nm with a 9×10^{19}cm^{-3} concentration of dopant. Finally, the substrate thickness is 50nm having a 1×10^{14}cm^{-3} concentration. A metal gate is implanted on the top of the device and the channel length is 6μm. The band gap of Ga_2O_3 is 4.8eV and electron affinity & mobility are 4.0eV and 118cm^2/V.s, respectively [36]. Accurate characteristics evaluation of Ga_2O_3 power device is crucial using modeling technique. SPICE parameters of Ga_2O_3 are extracted from TCAD using Shichman-Hodges model and summarized in Table 3.

TABLE 3. Extracted SPICE parameters for modeling Ga.

Model Parameter	Values
Length of channel (L)	6 μm
Width of channel (W)	4.7 ×10^6 μm
Oxide thickness (TOX)	20 nm
Bulk mobility (U0)	118 cm^2/V·s
Zero-bias threshold voltage (VTO)	−1.75 V
Substrate doping (NSUB)	2.0 ×10^{17} cm^{-3}
Transconductance parameter (KP)	46 ×10^{-6} A/V^2
Source-drain overlap (CGD)	4.30 ×10^{-11} F/m
Gate-source capacitance (CGS)	2.86 ×10^{-11} F/m

These parameters are used to model Ga_2O_3 power MOSFET in MATLAB using Simscape physical modeling SPICE NMOS model. N-Channel MOSFET (NMOS) used in Simscape modeling uses either Shichman-Hodges equations or surface-potential-based mode for MOSFET modeling [37]. The Shichman-Hodges equations for MOSFET modeling in linear and saturation modes are given below. The device I-V curve is observed and compared using the TCAD and MATLAB model as shown in figure 2.

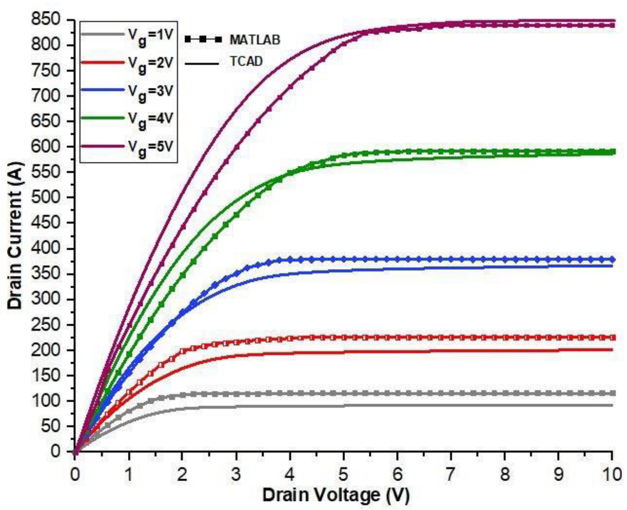

FIGURE 2. Ga_2O_3 **V-I curve using TCAD and MATLAB SPICE model.**

Linear mode MOSFET Drain current,

$$\mathbf{I_D}=\beta\{(\mathbf{V_{GS}}-\mathbf{V_{th}})\mathbf{V_{DS}}-{\mathbf{V^2_{DS}}}/{2}\}\,(1+\ell\mathbf{V_{DS}}) \tag{1}$$

Saturation mode MOSFET Drain current,

$$\mathbf{I_D}={\beta}/{2}(\mathbf{V_{GS}}-\mathbf{V_{th}})^2(\mathbf{1}+\ell\mathbf{V_{DS}}) \tag{2}$$

where, $\mathbf{V_{GS}}, \mathbf{V_{DS}}$ and $\mathbf{V_{th}}$ are gate to source, drain to source, and threshold voltages of MOSFET, respectively. 'β' is the gain factor-beta of the transistor and 'ℓ' is the channel modulation effect.

III. DESIGN OF PROPOSED Ga_2O_3 DEVICES BASED HIGH POWER EV FAST CHARGER

The research proposed a Fast DC charging station that will be able to deliver high power using ultra-wideband gap (UWBG) material power devices. Ga_2O_3 (UWBG) power devices based 500kW ($\approx 3 \times 165$ kW) capacity fast charger is designed for electric vehicle charging as shown in figure 3. The proposed charger is divided into two main sections: an AC-DC (PWM rectifier) converter with unity power factor control and an isolated DC-DC converter module performing a required rating charging function.

TABLE 4. Charging station grid parameters.

Symbol	Parameter	value
$\mathbf{P_g}$	Rated Grid Power	500kW (≈ 165kW× 3)
$\mathbf{V_g}$	Rated grid voltages (line-line, rms)	415V rms
$\mathbf{i_g}$	Rated grid current (line-line, rms)	1.15kA (289A each)
$\mathbf{f_g}$	Grid frequency	50 Hz
$\mathbf{R_{eq}}$	Grid equivalent resistance	0.008 Ohm
$\mathbf{L_{eq}}$	Grid equivalent inductance	0.016mH

Full bridge topology is used in DC-DC converter with a high-frequency transformer to obtain isolation [38]. Three separate interleaved DC-DC converter modules topology is used to design the 500kW power EV charger. Each module has a capacity of nearly 165kW and can deliver 100-950V & 0-200A charging voltages and current, respectively. The variety of output range makes it suitable for every kind of electric vehicle and for future E-buses or heavy transport vehicles (HTV). Detailed design analysis for the 165kW charger module is discussed and analyzed below. Grid parameters are summarized in Table 4.

Three-phase bi-directional power converters can perform both grid-to-vehicle (G2V) and vehicle-to-grid (V2G) operations. The bi-directional converter links the high-power AC bus with the DC bus and controls the power flow from both directions. It will work as a rectifier for AC-DC flow (rectification mode) and act as a DC-AC converter (inversion mode) to the power grid from the DC bus. High switching frequency reduces the filter and transformer size which results in a decrease in overall station weight. PI controller is used to controlling the DC-bus voltages and charging power of the EV battery. The charger module uses constant current and constant voltage (CC-CV) mode for battery charging. This method will reduce the heating effect, improve the charging time, and accomplish stable fast charging of the station.

Ga_2O_3 power MOSFETs are driven by gate drivers which are controlled by separate AC/DC and DC/DC controllers. Figure 4 represents the overall diagram of the charging station including AC/DC and DC/DC power converters with control & power signals.

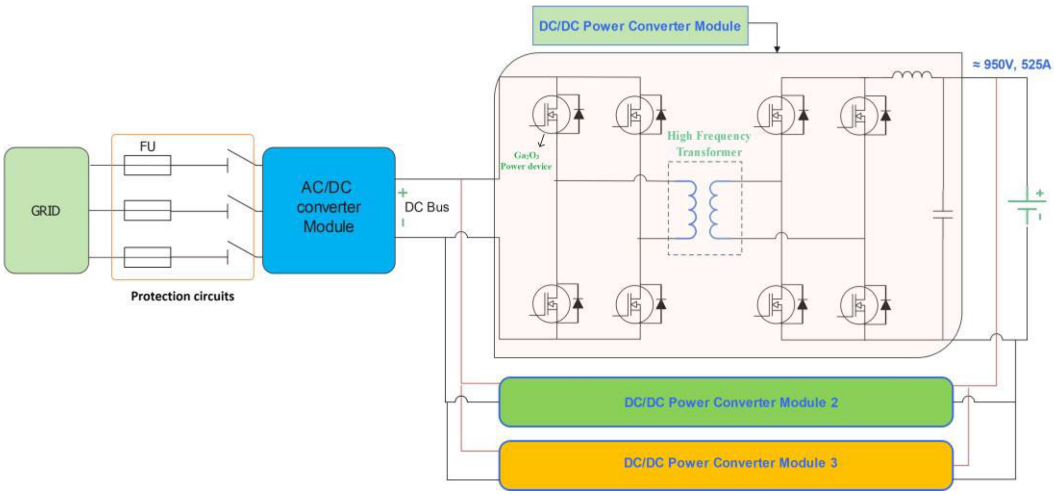

FIGURE 3. High Power DC ultra-fast EV charger topology.

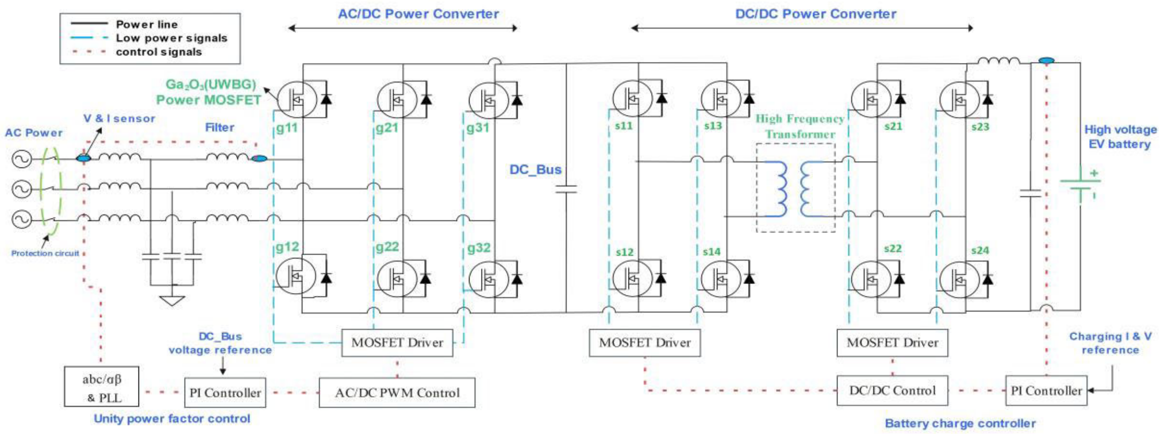

(a)

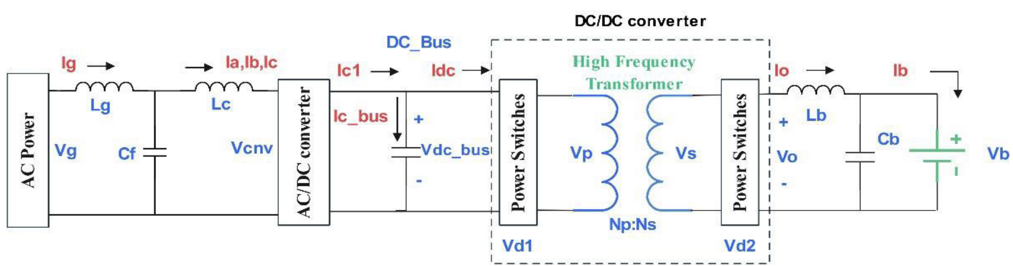

(b)

FIGURE 4. Ga_2O_3 Power devices-based EV fast charger design (a) schematic diagram of the EV charger using bidirectional converters (b) single phase equivalent EV fast charger diagram.

A. LCL FILTER DESIGN

The input LCL filter between grid and AC/DC converter reduces harmonics and is helpful to achieving unity power factor at the grid side using PWM control. The open transfer function of grid current (Ig) to AC-DC converter and grid voltage (Vg) is expressed in the following equations in the Laplace domain denoted as Gc(s) and Gg(s), respectively [39], [40].

$$G_c(s) = \frac{1}{s\left(L_g + L_c\right) + s^3 L_g L_c C_f} \tag{3}$$

$$[3pt]G_g(s) = \frac{s^3 l_c C_f + 1}{s\left(L_g + L_c\right) + s^3 L_g L_c C_f} \tag{4}$$

where $\mathbf{L_g}$, $\mathbf{L_c}$, and $\mathbf{C_f}$ are grid side inductor, converter side inductor, and filter capacitor, respectively. According to the above transfer function equations the resonance frequency ($\boldsymbol{\omega_{res}}$) exist in the system is calculated as below.

$$\omega_{res} = \sqrt{\frac{L_g+L_c}{L_g L_c C_f}} \tag{5}$$

According to the design criteria for LCL filter design given in papers [41], [42], and [43] following equations (eq. 6 & eq. 7) are used to find proper filter values. In this research, a charger is designed for a maximum of 10% current attenuation for the AC/DC converter ($\mathbf{\Delta i_{max} \approx 30}A$). The value of filter inductors ($\mathbf{L_g \& L_c}$) for modulation index ($\mathbf{m_a}$)range $\mathbf{0.6 - 0.95}$ is calculated below according to the parameters given in Table 5 [40].

$$L_c = \frac{V_{DC\_bus}\,(2 - m_a)}{4 f_{s1}\,\Delta i_{max}} \approx 0.7\text{mH to } 1.0\text{mH} \approx L_g \tag{6}$$

TABLE 5. EV Fast charger design parameters.

Parameter	Values
V_DC bus voltages	800 V
AC/DC current attenuation Δi_max	30A max
Full bridge DC/DC converter duty ratio (D)	0.95 max
PWM converter modulation index (m_a)	0.95 max
AC/DC converter switching frequency f_{s1}	10kHz
DC/DC converter switching frequency f_{s2}	50kHz
DC/DC converter output current ripple ΔI	1A
DC/DC converter output voltage ripple ΔV	1V
LCL Filer values (L_g, L_c, C_f)	$L_g, L_c = 0.8\text{mH}, C_f = 12\mu\text{F}$
Output filter (L_b, C_b)	2mH, 10μF

While designing the filter capacitor of the LCL filter total reactive power of the converter should be limited at grid frequency. The maximum capacitor value (C_f) for 165kW power should be approximately 50μF as calculated below. The typical value of the reactive power coefficient (λ) is normally in the range of 0.05 to 0.1 (λ =0.05).

$$C_f(\max) = \frac{\lambda P_g}{2\pi f_g \left(V_g\sqrt{3}\right)^2} \approx 50\mu F \tag{7}$$

LCL resonance frequency according to equation (eq. 5) by selecting Cf=12μF is 14.4kHz. The filter values computed in the above formulas satisfied the equations given below according to the LCL filter design procedure.

$$\mathbf{10\omega_g \le \omega_{res} \le 0.5\ \omega_{sw1}} \tag{8}$$

B. BI-DIRECTIONAL AC/DC POWER CONVERTER

Three phase bi-directional power converter also named PWM rectifier is a well-known converter to achieve desired DC bus voltage by a feedback control loop. Connecting an AC grid power with a DC system by using uncontrolled rectifiers established unwanted distortion in current and voltages at the grid side. PWM rectifier produces a nearly sinusoidal current at the source side and with the power factor (PF) control technique unity PF at the grid side can be achieved. From figure 4b the grid voltages can be equated with AC/DC converter voltages in the following terms by neglecting the filter capacitor [39].

$$V_g(t) = R_t i_g(t) + L_t \frac{d}{dt} i_g(t) + V_{cnv}(t) \tag{9}$$

Here Rt and Lt are total resistance and inductance, respectively, from the grid to AC/DC converter ($R_t \approx 0$). The output current of the AC/DC power converter in terms of the upper power switching function ($g_{11}, g_{21} \& g_{31}$) and DC-bus current is defined as,

$$I_{c1} = g_{11} I_a + g_{21} I_b + g_{31} I_c \tag{10}$$

$$I_{dc} = I_{c1} - C_{bus} \frac{d}{dt} V_{DC\_bus} \tag{11}$$

Using abc/$\alpha\beta$/dq transform reference frame PWM converter equation in dq-frame in rectification mode is equated in the following equations.

$$V_{c\_d} = L\frac{di_{gd}}{dt} - \omega L i_{gq} + V_{gd} \tag{12}$$

$$V_{c\_q} = L\frac{di_{gq}}{dt} + \omega L i_{gd} + V_{gq} \tag{13}$$

where, i_{gd}, i_{gq}, V_{gd} and V_{gq} are grid current and voltages in dq-frame and V_{c_d}, V_{c_q} are PWM rectifier terminal voltages. PWM rectifier has dual control loops, the outer loop is known as the DC voltage loop and the inner is named as the current loop. Inner loops (current loops) control the 'd' and 'q' axis current of the converter through which active and reactive power flow is regulated.

C. BI-DIRECTIONAL DC/DC POWER CONVERTER

DC/DC Full bridge power converter topology is used to connect DC-bus with the EV battery. The power converter controls the wide range of charging voltage from 100 to nearly Vdc-bus along with current control. A fully controlled power switch on both the primary and secondary sides makes it a bidirectional power converter. A High-frequency transformer (HFT) provides galvanic isolation between the charger and battery. Ga_2O_3 power devices can switch at high frequency at fewer losses with proper biasing and complementary circuits as compared to the same power Si-based IGBT/MOSFET. The switching frequency of the DC/DC converter is selected 50kHz (f_{s2}) by considering the frequency limitations of available high-power HFT. Assume the voltage drop of the Ga_2O_3 power devices of the primary and secondary side of HFT is V_{d1} and V_{d2}, respectively. The output voltage of the DC/DC converter is formulated below [44].

$$V_o = \left\lfloor \left(V_{DC_{bus}} - 2V_{d1}\right)\frac{N_s}{N_p} - 2V_{d2} \right\rfloor \frac{2T_{on}}{T_{sw2}} \tag{14}$$

$N_p \& N_s$ are primary and secondary turn ratios of HFT(1:1). By neglecting the switching device and HFT losses the output current of the DC/DC converter by equations 10 & 11 is defined as,

$$I_o \approx I_{dc} \approx (g_{11}I_a + g_{21}I_b + g_{31}I_c) - C_{bus}\frac{d}{dt}V_{DC\_bus} \quad (15)$$

D. OUTPUT FILTER DESIGN

The high-frequency pulsating output of the full bridge DC/DC converter is filtered using LC filter. Assume the current (ΔI) and voltage (ΔV) ripple of the DC converter is approximately 1A&1V, respectively. The battery voltages are approximately equal to the DC/DC converter output ($V_b \approx V_o \approx DV_{DC_{bus}}$) by neglecting losses. LC output Filter values of the converter are evaluated from the following equations (Duty = 0.5-0.95) [45].

$$T = \frac{1}{F_{sw2}} = T_{on} + T_{off} = \frac{\Delta IL_b}{V_o - V_b} + \frac{\Delta IL_b}{V_b} \quad (16)$$

$$L_b = \frac{V_{DC\_bus}D(1-D)}{F_{sw2}\Delta I} \approx 0.76\text{mH to } 4\text{mH} \quad (17)$$

$$C_b = \frac{V_{DC\_bus}D(1-D)}{8L_bF_{sw2}^2\Delta V} \approx 2\mu\text{F to } 10\mu\text{F} \quad (18)$$

IV. SIMSCAPE PHYSICAL MODELING

A. DESIGN CONSIDERATIONS

The detailed and extensive simulation model of a proposed Ultra-fast EV charger is designed on the Simscape physical modeling tool (MATLAB). The complete EV charger model contains many blocks and subsystems, like Power systems, SPICE power converters, driver circuits, control systems, physical components, battery model etc. The Backward Euler's method is used for the Simscape simulation modeling solver (MATLAB), which solves one or more ordinary differential equations (ODE) using the Euler method by setting a fixed step size of 1e-6 seconds (sampling rate). The simulation analysis is performed on a Li-Ion 100kWh capacity battery (nearly the same capacity is used in the latest 2022 EV e.g., Mercedes EQS, Ford Mustang Mach-E, Tesla Model S, etc.)

B. SIMULATION MODEL AND RESULTS

Physical modeling of EV chargers is performed using Simscape (MATLAB) to verify the theoretical design and above calculations. The Block model of a high-power fast EV charger based on subsystem is shown in figure 5 and system parameters are summarized in Table 6. MATLAB Simscape enables you to rapidly create models of physical systems within the Simulink environment [46]. Simscape helps build physical power converter models based on physical connections and configurable SPICE models which effectively provide the designed system's dynamic response [47].

The dynamic behavior of Ga_2O_3 Power MOSFET is verified by comparing characteristic analysis of the MOSFET model with Salvico TCAD as shown previously in figure 2. Ga_2O_3 power MOSFET module used in Simscape physical power converters modeling with the characteristic curve is shown in figure 6. Three-phase Ga_2O_3-based bidirectional

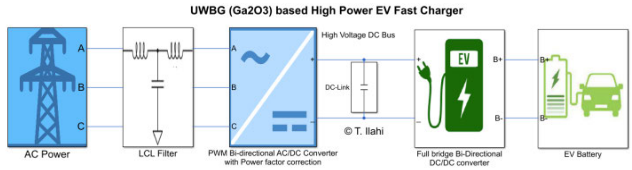

FIGURE 5. Simscape MATLAB model of UWBG high power EV fast charger.

TABLE 6. EV charger Simulation Design Specifications.

Sr.	Parameter	Specification/Range
1	Output Power	165 kW max.
2	Output voltage	950V max.
3	Output current	200A max.
4	Input	380-415V f=50Hz
5	Operating Frequencies	10 kHz and 50kHz
6	Sampling Time	1e-6 seconds
7	Gate voltage	10V
8	Driver Propagation Delay (HL-LH)	20ns

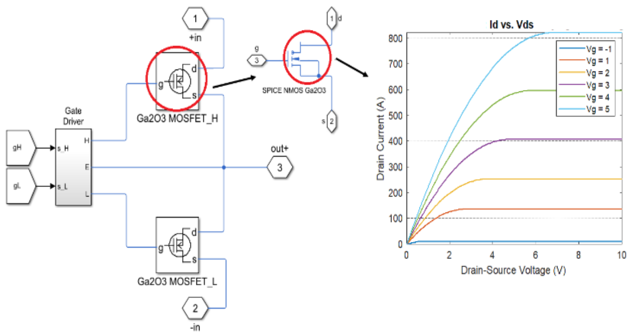

FIGURE 6. Ga_2O_3 Power MOSFET module with the characteristic curve.

AC-DC converter topology connects the AC grid with the DC voltage bus. A DC capacitor is connected across DC-bus to provide better voltage regulation. The bidirectional AC-DC converter can operate in two modes, rectification and inversion mode which is useful for grid-to-vehicle and vehicle-to-grid power transfer.

In simulation only rectification mode is discussed which is charging of high voltage EV battery from gird. Figures 7 & 8 show the grid three-phase V & I response and DC-bus voltage behavior. The total harmonic distortion (THD) response of the systems at the fundamental frequency of 50Hz is presented in figure 7(c). Steady-state behavior is achieved within 0.15s of charging and starting overcurrent can be reduced from the current limiting protection devices.

The unity power factor control is applied in simulation using the phase-lock loop (PLL) technique and by abc/$\sigma\beta$ & $\sigma\beta$/dq transforms. The d-axis in the d-q coordinate system controls the active power (P) and q-axis represents the reactive power (Q). To achieve a unity power factor, the reference value of the reactive power current is set to zero (i_{gq} =0) and

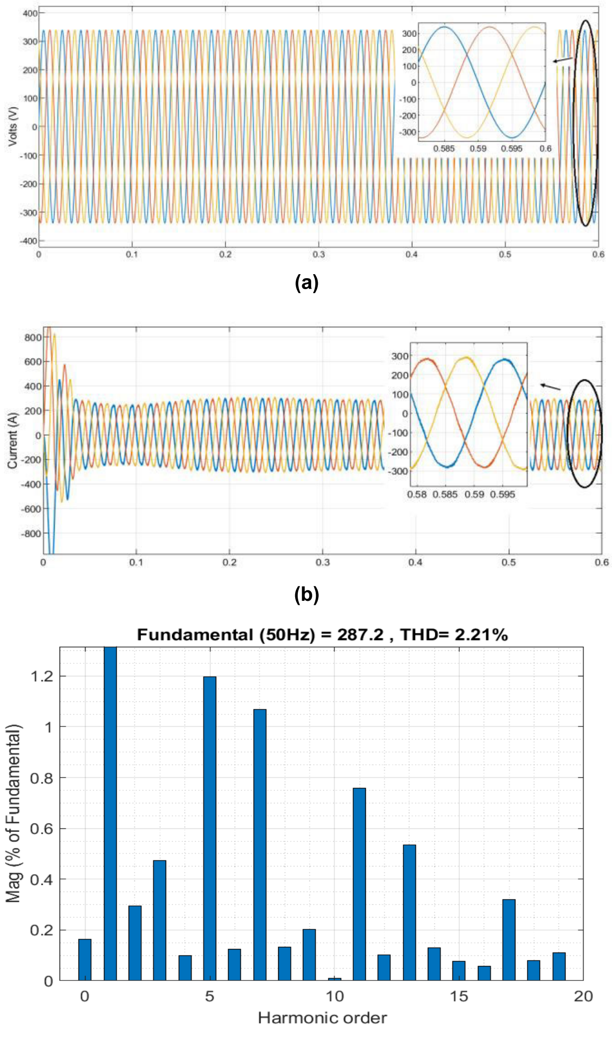

FIGURE 7. Grid three-phase voltage and current response during EV battery charging (a) Grid three-phase voltages (b) Grid three-phase current (c) Total harmonic distortion (THD).

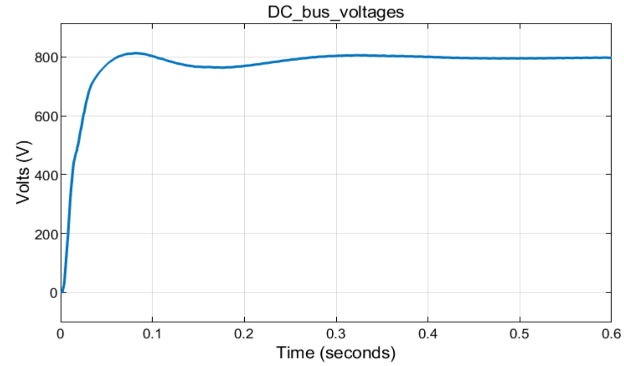

FIGURE 8. High voltage DC-bus voltage response.

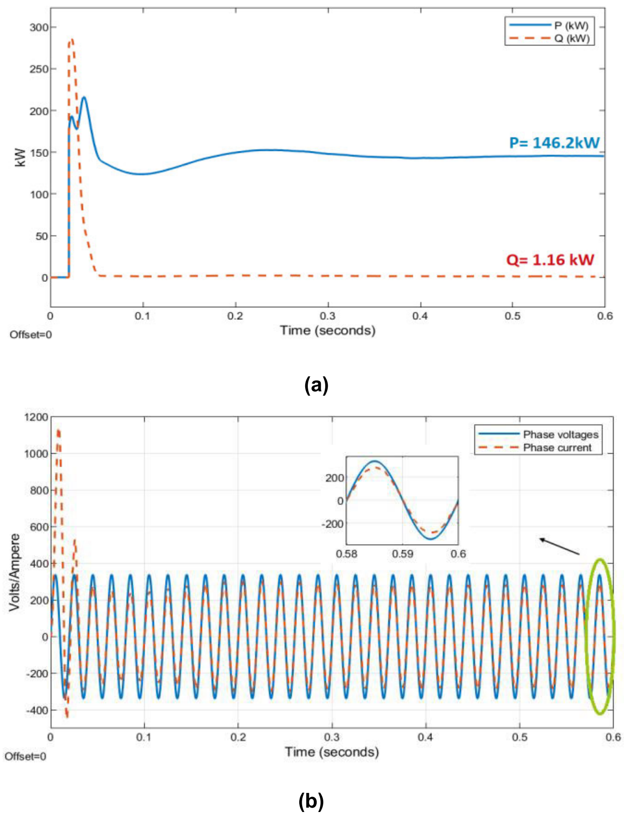

FIGURE 9. Power Grid unity power factor control (a) Grid active and reactive power (b) Grid phase voltage and current.

the PWM rectifier starts operating in a unity power factor state. Grid active and reactive power with phase voltage & current response is shown in figure 9.

The full-bridge topology of the DC/DC converter is used to connect the DC bus and battery pack. The output filter circuit consists of inductor L_b and capacitor C_b. The DC bus voltage and current of the EV station is the main control object. Therefore, the most widely used control strategy, the voltage outer-loop, and current inner-loop double PI control are applied in this simulation. The maximum charging current is set to 200A for the charging port during constant current (CC) operation for a bulk mode of charging as shown in figure 10. In the simulation, only bulk mode constant current charging is observed using high-power Ga_2O_3 power devices.

Dynamic performance of EV fast charger using Simscape model illustrates the correct response of both AC/DC & DC/DC power converter using Ga_2O_3 power devices. The system starts stable charging of high voltage EV battery within 0.15s using dual separate active control systems. EV battery initial state of the charger (SOC) is 20% the charging response over 0.6s is observed in figure 11. The proposed charger can charge a 100kWh capacity EV battery within 10 minutes up to 80% SOC. Whereas, approximately 100kWh capacity EV vehicle will charge in 15 to 45 minutes from the currently available DC fast charger. Nearly 30% of charging time will be reduced from the proposed EV charger.

The accurate measurement of the total charging time of the battery needs a sophisticated algorithm. The simplified equation to estimate the charging time of the charger is given

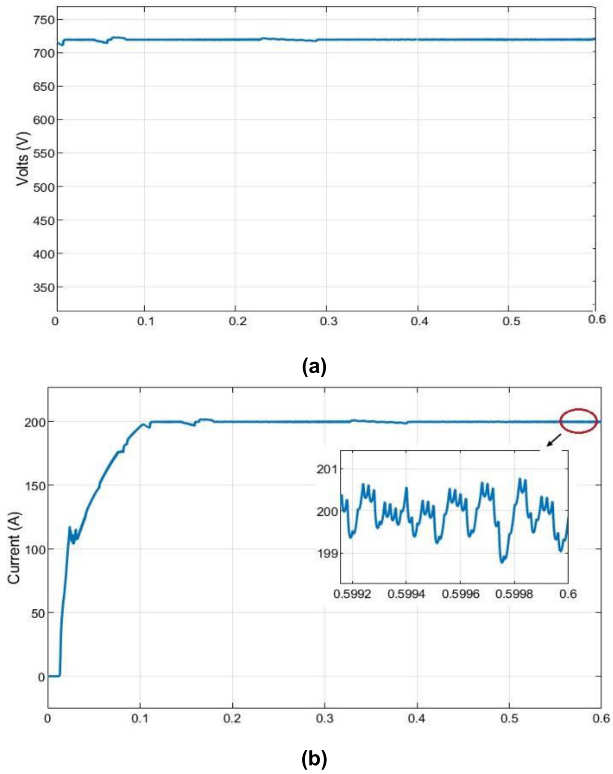

FIGURE 10. Constant current (CC) bulk mode charging response of high voltage EV battery (a) charging voltages (b) charging current.

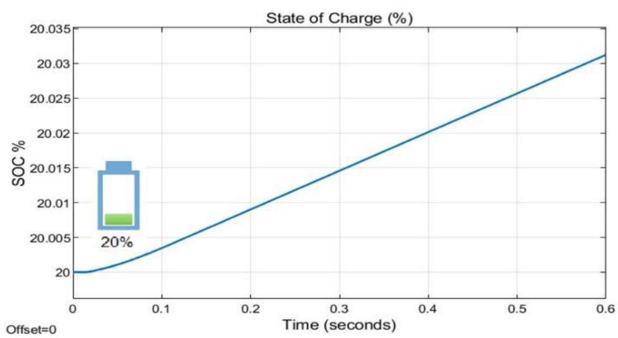

FIGURE 11. EV battery charging response.

below [48],

$$\mathbf{t_{charger}}=\frac{\mathbf{B_{cap}}\times(1-\mathrm{SOC})}{\mathbf{P_{charger}}} \tag{19}$$

where, B_{cap} is capacity of EV battery and $P_{charger}$ defines the EV charger power. The latest EV model like the Mercedes EQS, Ford Mustang Mach-E, Tesla Model S, etc. has a battery capacity of 100kWh. The total estimated speed of charging a 100kWh battery from 0 to 100% is approximately 12 minutes.

V. POWER LOSS AND COMPARATIVE ANALYSIS

In this section Ga_2O_3 device conduction and switching, loss is evaluated, and Proposed EV charger parameters are compared with commercially available DC fast charger. Maximum power losses in semiconductor devices (Power diode, MOSFET, IGBT, etc.) depend on the conduction and switching behavior of the device. Power losses analysis of the power MOSFETs is an important factor to investigate the performance of the device. Conduction losses depend on the 'ON' state resistance and duty cycle (D) of MOSFET while switching losses occurs during the transition between 'ON' and 'OFF' state of the device. For high-voltage applications, conduction and switching losses are important factors of power converters. Equations used for losses and efficiency evaluation of converters are given below [49], [50].

$$P_{semiconductorloss} = P_{conduction}+P_{switch} \tag{20}$$

$$P_{conduction} = DI_D^2R_{on-state} \tag{21}$$

$$P_{switch} = E_{Total} \times F_{sw} \tag{22}$$

$$E_{Total} = E_{on} + E_{off}=\frac{1}{2}V_{ds}I_D\left(t_{i_{rise}} + t_{V_{fall}}\right) + \frac{1}{2}V_{ds}I_D\left(t_{i_{fall}} + t_{V_{rise}}\right) \tag{23}$$

Here, $\mathbf{t_{i_{rise}}}, \mathbf{t_{V_{rise}}} \& \mathbf{t_{i_{fall}}}, \mathbf{t_{V_{fall}}}$ are rise and fall times of MOSFET current and voltage while switching. Eon & Eoff are energy losses during MOSFET On and Off. Figure 12 and 13 shows the switching and conduction losses of Ga_2O_3 power device, respectively. Conduction loss of Ga_2O_3 power device is less compared to Silicon carbide (SiC) MOSFET (C3M0021120K) as shown in figure 12 (Tj=25°C, VDD= 800V) which makes it suitable for high current applications.

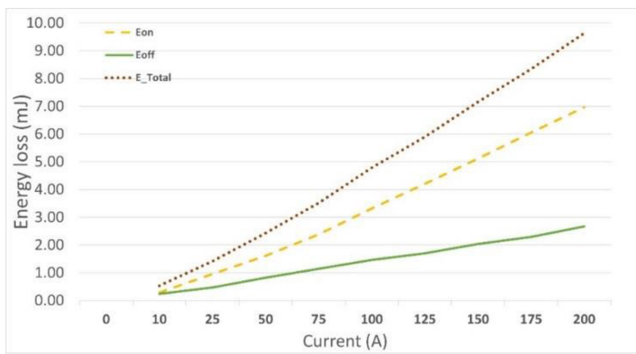

FIGURE 12. Switching loss of Ga_2O_3 power devices (VDD= 800V).

The EV converter efficiency of the system as per figures 8 & 9 and loss analyses is nearly 98.55%. The present high-frequency transformers are more than 99.5% efficient [51]. By including HFT losses proposed charger efficiency is greater than 98% which is higher than the available DC fast charger (380 – 480V input). The comparative analysis of the designed DC fast charger in terms of capacity, efficiency, ratings, power factor, and THD (total harmonics distortion) is present in Table 7 (Some technical details are not declared by the charger manufacturing company which are listed with dash lines).

The research successfully designed the Ga_2O_3 (UWBG) material-based high current density EV ultra-fast charger

TABLE 7. Comparison of EV DC fast charger and proposed model (3-phase 380 – 480 V input supply).

Sr	DC fast Charger model	Max Capacity	V/I ratings	η	P.f	Losses	THD
1	NEX2 SEED180 [55] DC fast charger	180kW	150–1000V, 350A	93.5%	0.99	< 7%	< 5%
2	ABB's Terra HP [56] Ultra-fast charger	350kW	150 – 920 V, 500A	95%	> 0.97	< 6%	< 8%
3	Tesla [28] Supercharger	135 kW	50–410 V, 330A	92%	> 0.97	< 9%	---
4	EVTEC [28] Espresso & charge	150 kW	170–500 V, 300A	93%	> 0.97	< 8%	---
5	EVSE Tritium [57] DC fast charger	50kW	50–500 V, 125A	>92%	0.99	< 9%	---
6	**Proposed** Ultra-fast charger	500kW	100-950 V, 525A	>98%	0.99	< 3%	< 3%

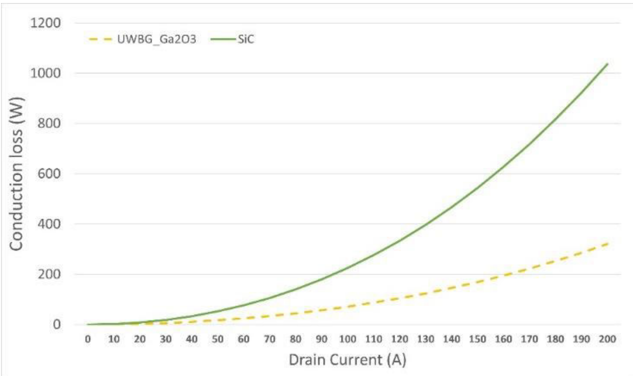

FIGURE 13. Conduction loss comparison of Ga_2O_3 and SiC power MOSFET.

with improved efficiency. Device modeling of the Ga_2O_3 material power device is performed by the Silvaco TCAD tool. Complete model description in terms of dimension, material characteristics, doping concentration, and parameter extraction is presented in the paper. Trace in figure 2 verifies the MATLAB (SPICE NMOS block model of Ga_2O_3) with the results obtained from the Silvaco TCAD software tool. The extracted results validate the design procedure of the LCL input filter, output filter, mathematical equations of the converter, and model design parameters. All power electronics devices like power diodes, power transistors (BJT, IGBT, or MOSFET), etc. have energy losses in terms of conduction and switching. The mathematical expressions to evaluate losses are explained in section V. The comparison with commercially available wide bandgap (WBG) technology-based SiC MOSFET (C3M0021120K) is also performed to validate the core objective of increased efficiency with the same testing conditions.

The fast-trending improvement in battery technologies like Lithium-Sulfur batteries, Solid-state batteries, cobalt-free batteries, etc. has high current density and better state of health (SOH) as compared to current battery technology. The proposed ultra-fast charger will also be able to charge upcoming EVs battery (capacity larger than 100kWh). The limitation of the system which causes instability or poor power factor (PF) & total harmonic factor (THD) is improper selection of filter values, extreme thermal limits, frequency limitation of an isolated transformer, extremely high switching frequencies etc. The filter value ($\mathbf{C_f}, \mathbf{L_g}, \mathbf{L_c}$) should satisfy the equations (eq.5, eq.7, and eq.8). DC/DC converter higher duty cycle (> 0.95) and saturation of high-frequency transformer (HFT) can also lead the system toward instability. The signal-piloted and optimization tools can enhance computational effectiveness and real-time compression [52], [53], [54]. The feasibility of incorporating these tools in the suggested assessment method can be investigated in the future.

VI. CONCLUSION

The research provides the new Ga_2O_3 power devices based high power Ultra-fast charger using a bi-directional power converter. The proposed solution improves the charging infrastructure power capacity, efficiency and reduces charging time. Research proves that the efficiency of high-capacity power converters increases up to more than 98% by using UWBG power devices. High electric field density, switching ability, current density with low leakage current, and forward voltage drop provide a new market for Ga_2O_3 power devices. The proposed solution resolves the complexity of charging for currently available or future high-voltage EV batteries. A high breakdown voltage of nearly VB $>$ 8kV makes it perfectly suitable for directly grid-tie applications. The paper successfully presented the Ga_2O_3 power device response using TCAD and SPICE MATLAB model. Simscape physical modeling is convenient to study the dynamic behavior of UWBG-based DC fast chargers in the Simulink environment. Theoretical calculation and simulation analysis of both AC/DC and DC/DC power converters help implement and design different capacity EV chargers. The dual active power control of converters provides a wide range of charging power for a variety of EV service providers. A wide range of power control reduces the complexity of using different chargers. Mathematical equations provide an optimum solution for designing input & output filters with power factor control. The future Ga_2O_3 based power electronics devices reduce the overall weight, size, and cost of high-power electric vehicles charger. High-power capacity EV chargers are the solution for upcoming electric vehicles like the Tesla 200kWh battery capacity founder series.

ACKNOWLEDGMENT

The authors are grateful to the University of Engineering and Technology (UET), Riphah International University, Effat University, Bahria University, Najran University, and LINEACT-CESI, for technical support.

REFERENCES

[1] A. Damm, J. Köberl, F. Prettenthaler, N. Rogler, and C. Töglhofer, ''Impacts of +2 °C global warming on electricity demand in Europe,'' *Climate Services*, vol. 7, pp. 12–30, Aug. 2017, doi: 10.1016/j.cliser.2016.07.001.

[2] G. Town, S. Taghizadeh, and S. Deilami, ''Review of fast charging for electrified transport: Demand, technology, systems, and planning,'' *Energies*, vol. 15, no. 4, p. 1276, Feb. 2022, doi: 10.3390/en15041276.

[3] M. A. Abella and F. Chenlo, ''Photovoltaic charging station for electrical vehicles,'' in *Proc. 3rd World Conf. Photovolt. Energy Convers.*, May 2003, pp. 2280–2283.

[4] S. Habib, M. M. Khan, F. Abbas, A. Ali, M. T. Faiz, F. Ehsan, and H. Tang, ''Contemporary trends in power electronics converters for charging solutions of electric vehicles,'' *CSEE J. Power Energy Syst.*, vol. 6, no. 4, pp. 911–929, Dec. 2020, doi: 10.17775/CSEEJPES.2019.02700.

[5] M. R. Khalid, I. A. Khan, S. Hameed, M. S. J. Asghar, and J.-S. Ro, ''A comprehensive review on structural topologies, power levels, energy storage systems, and standards for electric vehicle charging stations and their impacts on grid,'' *IEEE Access*, vol. 9, pp. 128069–128094, 2021, doi: 10.1109/ACCESS.2021.3112189.

[6] S. Chakraborty, H.-N. Vu, M. M. Hasan, D.-D. Tran, M. E. Baghdadi, and O. Hegazy, ''DC–DC converter topologies for electric vehicles, plug-in hybrid electric vehicles and fast charging stations: State of the art and future trends,'' *Energies*, vol. 12, no. 8, p. 1569, Apr. 2019, doi: 10.3390/en12081569.

[7] T. Gnann, S. Funke, N. Jakobsson, P. Plötz, F. Sprei, and A. Bennehag, ''Fast charging infrastructure for electric vehicles: Today's situation and future needs,'' *Transp. Res. D, Transp. Environ.*, vol. 62, pp. 314–329, Jul. 2018, doi: 10.1016/j.trd.2018.03.004.

[8] N. Sujitha and S. Krithiga, ''RES based EV battery charging system: A review,'' *Renew. Sustain. Energy Rev.*, vol. 75, pp. 978–988, Aug. 2017, doi: 10.1016/j.rser.2016.11.078.

[9] M. Yilmaz and P. T. Krein, ''Review of battery charger topologies, charging power levels, and infrastructure for plug-in electric and hybrid vehicles,'' *IEEE Trans. Power Electron.*, vol. 28, no. 5, pp. 2151–2169, May 2013, doi: 10.1109/TPEL.2012.2212917.

[10] M. Muratori, E. Kontou, and J. Eichman, ''Electricity rates for electric vehicle direct current fast charging in the United States,'' *Renew. Sustain. Energy Rev.*, vol. 113, Oct. 2019, Art. no. 109235, doi: 10.1016/j.rser.2019.06.042.

[11] J.-H. Kim, I.-O. Lee, and G.-W. Moon, ''Analysis and design of a hybrid-type converter for optimal conversion efficiency in electric vehicle chargers,'' *IEEE Trans. Ind. Electron.*, vol. 64, no. 4, pp. 2789–2800, Apr. 2017, doi: 10.1109/TIE.2016.2623261.

[12] A. R. Bhatti, Z. Salam, M. J. B. A. Aziz, and K. P. Yee, ''A comprehensive overview of electric vehicle charging using renewable energy,'' *Int. J. Power Electron. Drive Syst.*, vol. 7, no. 1, p. 114, Mar. 2016, doi: 10.11591/ijpeds.v7.i1.pp114-123.

[13] J. P. Christophersen, ''U.S. department of energy vehicle technologies program: Battery test manual for plug-in hybrid electric vehicles,'' U.S. Dept. Energy Nat. Lab., Battelle Energy Alliance, ID, USA, Manual Rep. INL/EXT-15-34184, 2014, doi: 10.2172/1169249.

[14] M. Budhia, G. A. Covic, J. T. Boys, and C.-Y. Huang, ''Development and evaluation of single sided flux couplers for contactless electric vehicle charging,'' in *Proc. IEEE Energy Convers. Congr. Expo.*, Sep. 2011, pp. 614–621, doi: 10.1109/ECCE.2011.6063826.

[15] M. Etezadi-Amoli, K. Choma, and J. Stefani, ''Rapid-charge electric-vehicle stations,'' *IEEE Trans. Power Del.*, vol. 25, no. 3, pp. 1883–1887, Jul. 2010, doi: 10.1109/TPWRD.2010.2047874.

[16] S. Bae and A. Kwasinski, ''Spatial and temporal model of electric vehicle charging demand,'' *IEEE Trans. Smart Grid*, vol. 3, no. 1, pp. 394–403, Mar. 2012, doi: 10.1109/TSG.2011.2159278.

[17] F. He, D. Wu, Y. Yin, and Y. Guan, ''Optimal deployment of public charging stations for plug-in hybrid electric vehicles,'' *Transp. Res. B, Methodol.*, vol. 47, pp. 87–101, Jan. 2013, doi: 10.1016/j.trb.2012.09.007.

[18] R. Collin, Y. Miao, A. Yokochi, P. Enjeti, and A. von Jouanne, ''Advanced electric vehicle fast-charging technologies,'' *Energies*, vol. 12, no. 10, p. 1839, May 2019, doi: 10.3390/en12101839.

[19] M. Yilmaz and T. Philip Krein, ''Review of charging power levels and infrastructure for plug-in electric and hybrid vehicles,'' in *Proc. IEEE Int. Electr. Vehicle Conf. (IEVC)*, Mar. 2012, pp. 1–8, doi: 10.1109/IEVC.2012.6183208.

[20] V. A. Boicea, ''Energy storage technologies: The past and the present,'' *Proc. IEEE*, vol. 102, no. 11, pp. 1777–1794, Nov. 2014, doi: 10.1109/JPROC.2014.2359545.

[21] J. Traube, F. Lu, D. Maksimovic, J. Mossoba, M. Kromer, P. Faill, S. Katz, B. Borowy, S. Nichols, and L. Casey, ''Mitigation of solar irradiance intermittency in photovoltaic power systems with integrated electric-vehicle charging functionality,'' *IEEE Trans. Power Electron.*, vol. 28, no. 6, pp. 3058–3067, Jun. 2013, doi: 10.1109/TPEL.2012.2217354.

[22] Z. Huang, Z. Li, C. S. Lai, Z. Zhao, X. Wu, X. Li, N. Tong, and L. L. Lai, ''A novel power market mechanism based on blockchain for electric vehicle charging stations,'' *Electronics*, vol. 10, no. 3, p. 307, Jan. 2021, doi: 10.3390/electronics10030307.

[23] G. Konstantinidis, F. Kanellos, and K. Kalaitzakis, ''A simple multi-parameter method for efficient charging scheduling of electric vehicles,'' *Appl. Syst. Innov.*, vol. 4, no. 3, p. 58, Aug. 2021, doi: 10.3390/asi4030058.

[24] D. S. Abraham, R. Verma, L. Kanagaraj, S. R. G. T. Raman, N. Rajamanickam, B. Chokkalingam, K. Marimuthu Sekar, and L. Mihet-Popa, ''Electric vehicles charging stations' architectures, criteria, power converters, and control strategies in microgrids,'' *Electronics*, vol. 10, no. 16, p. 1895, Aug. 2021, doi: 10.3390/electronics10161895.

[25] H. H. Coban, W. Lewicki, E. Sendek-Matysiak, Z. Łosiewicz, W. Drożdż, and R. Miśkiewicz, ''Electric vehicles and vehicle–Grid interaction in the Turkish electricity system,'' *Energies*, vol. 15, no. 21, p. 8218, Nov. 2022, doi: 10.3390/en15218218.

[26] S. Madhusoodhanan, A. Tripathi, D. Patel, K. Mainali, A. Kadavelugu, S. Hazra, S. Bhattacharya, and K. Hatua, ''Solid-state transformer and MV grid tie applications enabled by 15 kV SiC IGBTs and 10 kV SiC MOSFETs based multilevel converters,'' *IEEE Trans. Ind. Appl.*, vol. 51, no. 4, pp. 3343–3360, Jul. 2015, doi: 10.1109/TIA.2015.2412096.

[27] R. J. Kaplar, A. A. Allerman, A. M. Armstrong, M. H. Crawford, J. R. Dickerson, A. J. Fischer, A. G. Baca, and E. A. Douglas, ''Review—Ultra-wide-bandgap AlGaN power electronic devices,'' *ECS J. Solid State Sci. Technol.*, vol. 6, no. 2, pp. Q3061–Q3066, 2017, doi: 10.1149/2.0111702jss.

[28] S. Srdic and S. Lukic, ''Toward extreme fast charging: Challenges and opportunities in directly connecting to medium-voltage line,'' *IEEE Electrific. Mag.*, vol. 7, no. 1, pp. 22–31, Mar. 2019, doi: 10.1109/MELE.2018.2889547.

[29] X. Yan, I. S. Esqueda, J. Ma, J. Tice, and H. Wang, ''High breakdown electric field in β-Ga_2O_3/graphene vertical barristor heterostructure,'' *Appl. Phys. Lett.*, vol. 112, no. 3, Jan. 2018, Art. no. 032101, doi: 10.1063/1.5002138.

[30] M. H. Wong and M. Higashiwaki, ''Vertical β-Ga_2O_3 power transistors: A review,'' *IEEE Trans. Electron Devices*, vol. 67, no. 10, pp. 3925–3937, Oct. 2020, doi: 10.1109/TED.2020.3016609.

[31] M. Zhang, Z. Liu, L. Yang, J. Yao, J. Chen, J. Zhang, W. Wei, Y. Guo, and W. Tang, ''β-Ga_2O_3-based power devices: A concise review,'' *Crystals*, vol. 12, no. 3, p. 406, Mar. 2022, doi: 10.3390/cryst12030406.

[32] S. T. Meraj, N. Z. Yahaya, M. S. H. Lipu, J. Islam, L. K. Haw, K. Hasan, M. S. Miah, S. Ansari, and A. Hussain, ''A hybrid active neutral point clamped inverter utilizing Si and Ga_2O_3 semiconductors: Modelling and performance analysis,'' *Micromachines*, vol. 12, no. 12, p. 1466, Nov. 2021, doi: 10.3390/mi12121466.

[33] T. Razzak, H. Xue, Z. Xia, S. Hwang, A. Khan, W. Lu, and S. Rajan, ''Ultra-wide band gap materials for high frequency applications,'' in *IEEE MTT-S Int. Microw. Symp. Dig.*, Jul. 2018, pp. 17–19, doi: 10.1109/IMWS-AMP.2018.8457144.

[34] Y. Zhang and T. Palacios, ''(Ultra) wide-bandgap vertical power FinFETs,'' *IEEE Trans. Electron Devices*, vol. 67, no. 10, pp. 3960–3971, Oct. 2020.

[35] I. Lee, A. Kumar, K. Zeng, U. Singisetti, and X. Yao, ''Modeling and power loss evaluation of ultra wide band gap Ga_2O_3 device for high power applications,'' in *Proc. IEEE Energy Convers. Congr. Expo. (ECCE)*, Oct. 2017, pp. 4377–4382, doi: 10.1109/ECCE.2017.8096753.

[36] K. Ghosh and U. Singisetti, "Ab initio calculation of electron–phonon coupling in monoclinic β-Ga_2O_3 crystal," *Appl. Phys. Lett.*, vol. 109, no. 7, Aug. 2016, Art. no. 072102, doi: 10.1063/1.4961308.
[37] P. Yang, W. Ming, and J. Liang, "A step-by-step modelling approach for SiC half-bridge modules considering temperature characteristics," in *Proc. IEEE Energy Convers. Congr. Expo. (ECCE)*, Oct. 2020, pp. 2827–2834, doi: 10.1109/ECCE44975.2020.9235594.
[38] J. Han, X. Zhou, S. Lu, and P. Zhao, "A three-phase bidirectional grid-connected AC/DC converter for V2G applications," *J. Control Sci. Eng.*, vol. 2020, Jan. 2020, Art. no. 8844073, doi: 10.1155/2020/8844073.
[39] M. Liserre, F. Blaabjerg, and S. Hansen, "Design and control of an LCL-filter-based three-phase active rectifier," *IEEE Trans. Ind. Appl.*, vol. 41, no. 5, pp. 1281–1291, Sep./Oct. 2005, doi: 10.1109/TIA.2005.853373.
[40] F. Liu, X. Zhang, C. Yu, Z. Shao, W. Zhao, and H. Ni, "LCL-filter design for grid-connected three-phase PWM converter based on maximum current ripple," in *Proc. IEEE ECCE Asia Downunder*, Jun. 2013, pp. 631–635, doi: 10.1109/ECCE-ASIA.2013.6579165.
[41] K. Frisfelds and O. Krievs, "Design of a three-phase bidirectional PWM rectifier with simple control algorithm," *Latvian J. Phys. Tech. Sci.*, vol. 56, no. 3, pp. 3–12, Jun. 2019, doi: 10.2478/lpts-2019-0015.
[42] G. Majic, M. Despalatovic, and B. Terzic, "LCL filter design method for grid-connected PWM-VSC," *J. Electr. Eng. Technol.*, vol. 12, no. 5, pp. 1945–1954, 2017, doi: 10.5370/JEET.2017.12.5.1945.
[43] J. R. Rodriguez, J. W. Dixon, J. R. Espinoza, J. Pontt, and P. Lezana, "PWM regenerative rectifiers: State of the art," *IEEE Trans. Ind. Electron.*, vol. 52, no. 1, pp. 5–22, Feb. 2005, doi: 10.1109/TIE.2004.841149.
[44] A. Pressman, K. Billings, and T. Morey, *3-Half-and Full-Bridge Converter Topologies, Switching Power Supply Design*, 3rd ed. New York, NY, USA: McGraw-Hill, 2009, pp. 111–115. [Online]. Available: https://books.google.com.pk/books?id=RgV4zQEACAAJ
[45] D. Czarkowski, "10—DC–DC converters," in *Power Electronics Handbook*, M. H. Rashid, Ed., 4th ed. Oxford, U.K.: Butterworth-Heinemann, 2018, pp. 275–288, doi: https://doi.org/10.1016/B978-0-12-811407-0.00010-6.
[46] I. Tejado, D. Torres, E. Pérez, and B. M. Vinagre, "Physical modeling based simulators to support teaching in automatic control: The rotatory Pendulum," *IFAC-PapersOnLine*, vol. 49, no. 6, pp. 75–80, 2016, doi: 10.1016/j.ifacol.2016.07.156.
[47] B. Xu, L. Lu, and D. Gong, "Research on real-time simulation of power electronic circuits based on simscape," *J. Phys., Conf. Ser.*, vol. 2196, no. 1, Feb. 2022, Art. no. 012025, doi: 10.1088/1742-6596/2196/1/012025.
[48] J. A. Domínguez-Navarro, R. Dufo-López, J. M. Yusta-Loyo, J. S. Artal-Sevil, and J. L. Bernal-Agustín, "Design of an electric vehicle fast-charging station with integration of renewable energy and storage systems," *Int. J. Electr. Power Energy Syst.*, vol. 105, pp. 46–58, Feb. 2019, doi: 10.1016/j.ijepes.2018.08.001.
[49] G. Lakkas, "MOSFET power losses and how they affect power-supply efficiency," *Analog Appl.*, vol. 10, pp. 42–44, Apr. 2016.
[50] P. Varecha, P. Makyš, M. Sumega, and P. Sovička, "Power losses analysis in MOSFET 3-phase high current power inverter for automotive application area," *Transp. Res. Proc.*, vol. 40, pp. 571–578, Jan. 2019, doi: 10.1016/j.trpro.2019.07.082.
[51] Z. Guo, S. Sen, S. Rajendran, Q. Huang, X. Feng, and A. Q. Huang, "Design of a 200 kW medium-frequency transformer (MFT) with high insulation capability," in *Proc. IEEE Energy Convers. Congr. Expo. (ECCE)*, Oct. 2020, pp. 3471–3477, doi: 10.1109/ECCE44975.2020.9235985.
[52] S. M. Qaisar, "A two stage interpolator and multi threshold discriminator for the brain-PET scanner timestamp calculation," *Nucl. Instrum. Methods Phys. Res. A, Accel. Spectrom. Detect. Assoc. Equip.*, vol. 922, pp. 364–372, Apr. 2019, doi: 10.1016/J.NIMA.2019.01.004.
[53] S. M. Qaisar and F. Alsharif, "Signal piloted processing of the smart meter data for effective appliances recognition," *J. Electr. Eng. Technol.*, vol. 15, no. 5, pp. 2279–2285, Sep. 2020, doi: 10.1007/s42835-020-00465-y.
[54] A. Abbas, S. M. Qaisar, A. Waqar, N. Ullah, and A. A. A. Ahmadi, "Min-max regret-based approach for sizing and placement of DGs in distribution system under a 24 h load horizon," *Energies*, vol. 15, no. 10, p. 3701, May 2022, doi: 10.3390/en15103701.
[55] NEX2. *Charging Systems and Devices for Electric Vehicles: SEED 180*. Accessed: Nov. 14, 2022. [Online]. Available: https://docs.google.com/viewer?url=https%3A%2F%2Fwww.nex2.it%2Fs%2FSEED180-itaen.pdf
[56] ABB. *Electric Vehicle Infrastructure Terra High Power—GEN III Charger Ideally Suited for Highway*. Accessed: Nov. 14, 2022. [Online]. Available: https://search.abb.com/library/Download.aspx?DocumentID=9AKK107991A9632&LanguageCode=en&DocumentPartId=&Action=Launch
[57] EVSE Australia. *Tritium VEEFIL-RT DC Charger|50 kW*. Accessed: Nov. 14, 2022. [Online]. Available: https://evse.com.au/product/tritium-veefil-rt-dc-charger-50kw/

TEHSEEN ILAHI received the B.S. degree in electronics engineering from Sir Syed University of Engineering and Technology, Karachi, Pakistan, and the master's degree from the University of Engineering and Technology (UET), Lahore, Pakistan, in 2016, where he is currently pursuing the Ph.D. degree in electrical engineering. He is a Faculty Member with the Department of Electrical Engineering, Riphah International University, Lahore Campus, Pakistan. His research interests include electric vehicle charger design, power electronics converters, smart grids, analog and digital electronic circuits, and renewable energy technologies.

TAHIR IZHAR received the Ph.D. degree in power electronics from the University of Birmingham, U.K., in 1997. He was a Professor with the Department of Electrical Engineering, University of Engineering and Technology (UET), Lahore, Pakistan. He is currently the Research and Development Director with Maxell Power Pvt. Ltd., Lahore. His research interests include switch-mode power supplies, power electronics, analog and digital electronic circuits, power converters, and electrical machines. His research papers have been published in various foreign and local well-reputed journals.

SAEED MIAN QAISAR received the M.S. and Ph.D. degrees in electrical and computer engineering from the Institute National Polytechnic (INP) of Grenoble, Université Grenoble Alpes, France, in 2005 and 2009, respectively.

Subsequently, he did a postdoctoral stay at the INP of Bordeaux, France. Afterward, he held different research and development positions in France. He was an Associate Professor and a Researcher with the Department of Electrical and Computer Engineering, Effat University, Saudi Arabia. He is currently an Associate Professor and the Research Director with the LINEACT CESI, France. He has more than 200 research publications and holds two patents to his credit. His research interests include signal processing, circuits and systems, machine learning, smart grid, battery management systems, and sampling theory. He is on the technical review committee of several international conferences and journals. He is also serving as an editor for international journals.

UMAR TABREZ SHAMI received the bachelor's and master's degrees from the University of Engineering and Technology (UET), Lahore, Pakistan, and the Ph.D. degree from Tokyo, Japan, in 2010. He is currently working as an Associate Professor with the Department of Electrical Engineering, UET. His research interests include power converters, renewable energy technologies, power generation, and power system analysis.

MUHAMMAD ZAHID received the Ph.D. degree in electrical engineering from the Huazhong University of Science and Technology, China, in 2018. He is currently an Assistant Professor with the Department of Electrical Engineering, Riphah International University, Lahore, Pakistan. His research interests include FACTs devices, the reconfiguration of distribution systems, and smart grids.

ASAD WAQAR received the bachelor's degree in electrical engineering from the University of Engineering and Technology, Taxila (UET Taxila), in 2002, the master's degree in electrical power engineering from RWTH Aachen University, Aachen, Germany, and the Ph.D. degree in electrical power engineering from Huazhong University of Science and Technology, Wuhan, China, in 2016.

Before joining academia, he has vast industrial experience both locally and internationally. He is currently the Director of the Post Graduate Programs, Bahria University Head Office, Islamabad, Pakistan. He is a Professor with the Department of Electrical Engineering, Bahria University. He is actively involved in teaching and research activities. He has successfully supervised more than 50 M.S. and B.E.E. students. He has research collaborations with Oregon Tech, USA, Texas A&M University, USA, Huazhong University of Science and Technology, University of Malaya, Malaysia, King Saud University, Saudi Arabia, and Prince Sultan University, Saudi Arabia. He has research publications in many internationally reputed journals and conferences. His research interests include smart grids, microgrid operation and control, power quality, power electronics, network reinforcement planning, demand-side management, and big data analysis in power systems. He serves as a Reviewer for IEEE TRANSACTIONS ON POWER SYSTEMS, *Applied Energy*, *International Transactions on Electrical Energy Systems*, IEEE ACCESS, *Renewable and Sustainable Energy Reviews*, and *International Journal of Engineering Science and Technology*.

AHMAD ALZAHRANI received the Ph.D. degree from Missouri University of Science and Technology, Rolla, MO, USA, in 2018. He is currently an Assistant Professor with the Department of Electrical Engineering, Najran University, Najran, Saudi Arabia. He performs research in the areas of power electronic converters. His research interests include renewable energy applications, electric vehicles, energy harvesting, power management, wireless power systems, and power converters design and control.